Radiation Properties of Planar Antenna Arrays Based on Certain Categories of Aperiodic Tilings

Vincenzo Pierro, Vincenzo Galdi, *Senior Member, IEEE*, Giuseppe Castaldi, Innocenzo M. Pinto, *Member, IEEE*, and Leopold B. Felsen, *Life Fellow, IEEE*

***Abstract*—Two-dimensional *aperiodic tilings* are collections of polygons, devoid of any translational symmetries, capable of covering a plane without gaps and overlaps. Although *aperiodic*, these structures can exhibit *order* and *symmetry* in an extended sense. In this paper, we study the radiation properties of planar antenna arrays based on certain categories of two-dimensional aperiodic tilings that illustrate diverse aspects of aperiodic order. Background material on aperiodic tilings and their known electromagnetic properties is reviewed. Results are illustrated to highlight the effects of aperiodic order in the antenna array radiation properties. Potential applications are also envisaged.**

***Index Terms*—Antenna arrays, aperiodic tilings, radiation, quasi-crystals.**

I. Introduction

MANY applications in electromagnetics (EM) engineering involve the study of wave interaction with *ordered* structures. The simplest conceivable form of "order" is that associated with *periodicity*. In this connection, Floquet theory provides a rigorous and powerful framework, which has made possible the development of computationally effective and physically incisive characterizations and parameterizations of typical periodicity-induced wave phenomenologies. Recent advances in materials engineering have triggered a renewed interest in periodic structures, for designing frequency-selective surfaces, photonic bandgap (PBG) devices, artificial impedance boundaries, etc. (see, e.g., [1] and [2]). At the opposite extreme of the "order" scale are *random* geometries, which have been utilized for effective statistical modeling in applications like remote sensing and propagation in turbulent media and urban environments. Much less is known about the EM properties of geometries in the "gray zone" between *perfect periodicity* and *absolute randomness*.[1] This realm of "orderly disorder" encompasses a broad and still largely unexplored range of hierarchial order types, from "quasi-periodic" to "quasi-random." Traditionally, *aperiodicity* has been tied to the concept of *amorphousness*. However, the fairly recent discovery of "quasi-crystals," i.e., certain metallic alloys whose X-ray diffraction spectra exhibit unusual symmetries, has introduced new wrinkles into traditional concepts of "order" and "symmetry"; for example, five-fold symmetry is known to be *inconsistent* with spatial periodicity. Thus, suggestions that *aperiodicity* rather than periodicity might be the *generic* attribute of solid state have motivated studies of aperiodic structures from a different perspective. Particular interest has been shown in "aperiodic tilings," which consist of collections of polygons that cover a plane without gaps and overlaps and are devoid of any translational symmetries. Examples of such geometries, which arise in computational logic problems, have been known since the 1960s, but had been regarded as mathematical oddities. Although *aperiodic,* these geometries can still exhibit *order* and *symmetry* in a nontraditional sense (see [5]–[8] for an introduction to quasi-crystals and aperiodic tilings). In what follows, we shall use "quasi-crystal" to describe a rather general deterministic aperiodic arrangement, although the formal definition of the term is still not settled [9].

With a view toward exploring how aperiodic tilings might open up new options in EM engineering applications, we have recently initiated a sequential study of the EM properties of two-dimensional (2-D) versions of such geometries. In particular, we have chosen to look at the radiation from tiling antenna arrays, with the goal of determining how *local* and other *weak* forms of order and symmetry influence the radiation properties. Accordingly, we have selected a number of tiling geometries exhibiting various types and degrees of order and symmetry, from quasi-periodic to quasi-random. Although our main interest in this preliminary investigation is to understand basic properties and wave-dynamical phenomenologies, we have also included a *quantitative* parametric study of how various tilings affect directivity, sidelobe level, and bandwidth in radiated field observables. The rest of this paper is laid out as follows. Section II deals with the definition and parameterization of aperiodic tilings, and with illustration of characteristic features and the construction algorithms. Section III contains a compact review of known EM results on aperiodic-tiling geometries. Section IV is concerned with the study of the radiation properties of antenna arrays based on representative categories of aperiodic tilings. Brief conclusions are provided in Section V.

II. Perspectives on Aperiodic Tilings

A. Periodicity, Almost-Periodicity, and Aperiodicity

A 2-D *periodic* structure consists of an infinite repetition of a given *unit cell* according to a 2-D lattice

$$\mathbf{r}_{nm} = n\mathbf{p} + m\mathbf{q}, \quad n, m = 0, \pm 1, \pm 2, \ldots \tag{1}$$

Manuscript received April 14, 2004; revised July 19, 2004. The work of L. B. Felsen was supported in part by Polytechnic University, Brooklyn, NY 11201, USA.

V. Pierro, V. Galdi, G. Castaldi, and I. M. Pinto are with the Waves Group, Department of Engineering, University of Sannio, I-82100 Benevento, Italy (e-mail: pierro@unisannio.it; vgaldi@unisannio.it; castaldi@unisannio.it; pinto@sa.infn.it).

L. B. Felsen is with the Department of Electrical and Computer Engineering, Polytechnic University, Brooklyn, NY 11201 USA and also with the Department of Aerospace and Mechanical Engineering, Boston University, Boston, MA 02215 USA (e-mail: lfelsen@bu.edu).

Digital Object Identifier 10.1109/TAP.2004.841287

[1]A possible paradigm are *fractal* geometries, which do not fit these patterns but have found important applications in EM engineering (see [3], [4], and the references therein).

where $\mathbf{p}$ and $\mathbf{q}$ denote two basis vectors of the 2-D vector space $\mathbb{R}^2$. Depending on the unit cell geometry and on the lattice basis vectors $\mathbf{p}$ and $\mathbf{q}$, a periodic structure can also possess K-fold *rotational symmetry*, i.e., invariance with respect to rotations of angles $2\pi/K$ about a point (and thus, in view of translational invariance, about infinitely many points). For instance, square lattices with square unit cells give rise to two-fold and four-fold rotational symmetries. It is well known in crystallography [7], [8] that a 2-D periodic pattern cannot exhibit *arbitrary* rotational symmetries, irrespective of the unit cell geometry. The *crystallographic restriction* theorem [7], [8] states that the only possible rotational symmetries for a 2-D lattice are of order $K = 2, 3, 4$, or 6. Thus, for example, five-fold and eight-fold rotational symmetries are *not compatible* with spatial periodicity [7], [8].

To parameterize *aperiodicity*, perhaps the best known example is the class of "almost periodic functions" [10], i.e., functions that can be uniformly approximated by generalized Fourier series containing a countable infinity of *pairwise incommensurate* frequencies; if these frequencies are generated from a finite-dimensional basis, the function is typically called "quasi-periodic." The simplest one-dimensional (1-D) example of a quasi-periodic function can thus be written as

$$f(x) = \sin(x) + \sin(\gamma x) \tag{2}$$

where γ is an irrational number. Although this function is not periodic, there exist "almost translations" ξ (relatively dense in $\mathbb{R}$) such that, $\forall \epsilon > 0, |f(x) - f(x+\xi)| < \epsilon, \forall x \in \mathbb{R}$. It is interesting to note that this function can be viewed as the 1-D projection of a 2-D periodic function onto a line with irrational slope

$$f(x) = \sin(x) + \sin(y)|_{y=\gamma x}. \tag{3}$$

This observation is the basis of the so-called "cut and project" method, which permits generation of quasi-periodic point sets starting from higher dimensional periodic lattices (see Section II-B1). Quasi-periodicity represents only some of the mildest forms of aperiodicity. A somewhat broader view can be gained by studying *aperiodic tilings*.

B. 2-D Aperiodic Tilings

A 2-D "tiling" consists of an arrangement of polygonal shapes ("tiles") that covers a plane without overlaps or gaps; a tiling devoid of any translational symmetry is called *aperiodic*. Most of the 2-D concepts illustrated in this section can be generalized to three-dimensional (3-D) on replacing polygons by polyhedra. A tiling can be *decorated* by associating with each tile additional properties (e.g., a color); in what follows we shall only be concerned with *undecorated* tilings. The study of aperiodic tilings is interdisciplinary, involving branches of applied physics (crystallography, solid-state physics) and pure and applied mathematics (computational logic, discrete geometry, group theory, ergodic theory) [7], [8], [11]–[13]. Our presentation here is limited to emphasizing those qualitative and semi-quantitative aspects that explain the relevant wave physics and suffice for implementation of selected parametric studies pertaining to the radiation properties of tiling-based planar antenna arrays.

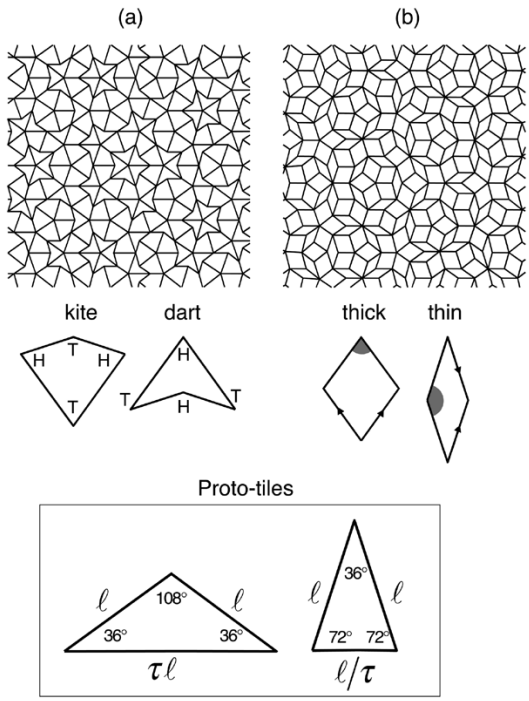

Fig. 1. *Penrose* tilings. (a) "Kite and dart" and (b) "Thick and thin." Both sets of tiles are obtained by proper juxtaposition of two isosceles triangles (see inset) with angles (36°, 36°, 108°) and (72°, 72°, 36°), respectively; $\tau = (1+\sqrt{5})/2$ is the golden mean. Two possible labeling schemes are shown for the matching rules that need to be enforced to prevent creation of periodic (or other uninteresting) patterns. For the *kite and dart* configuration, vertices marked with same letters ("H" or "T") must go together. For the *thick and thin* configuration, two adjacent vertices must both be blank or colored, and two adjacent edges must both be blank or both have an arrow pointing in the same direction.

The existence of *aperiodic sets*, i.e., sets of shapes capable of tiling a plane *only aperiodically,* was proved in the early 1960s within the framework of computational logic [14], [15]. From the first known aperiodic tiling, which consisted of more than 20 000 tile shapes [15], mathematicians were challenged to find ever simpler aperiodic sets. In 1974, Sir Roger Penrose, a British mathematical physicist at Oxford University, devised an aperiodic set consisting of just *two* tiles [16]. The corresponding tiling, named after him, is among the best known and most frequently studied aperiodic patterns. Examples are depicted in Fig. 1, with reference to its two most popular versions that came to be known as "kite and dart" [Fig. 1(a)] and "thick and thin" [Fig. 1(b)]. Although aperiodic, *Penrose* tilings display substantial order and symmetry, whose subtleties are discussed in Section II-B2. As shown in Fig. 1, both sets of tiles are derived by properly arranging two isosceles-triangle prototiles with internal angles (36°, 36°, 108°) and (72°, 72°, 36°), respectively. The scale that pervades the pattern is the golden mean $\tau = (1+\sqrt{5})/2$ ("most irrational" number [17]), which is the ratio of the areas in both sets of tiles [$\tau = A_1/A_2$, where A_1 is the area of a *kite (thick)* and A_2 is the area of a *dart (thin)*]. It has been proved that these sets of tiles can cover the plane aperiodically in infinitely many ways, but these can be distinguished only over an *infinite* plane (i.e., any arbitrarily large but finite region is inadequate to characterize the tiling completely) [8],

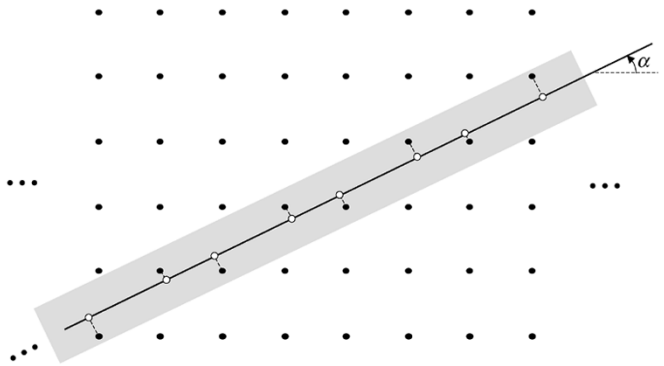

Fig. 2. Schematic illustration of the "cut and project" method in 1-D. A 2-D square lattice (black circles) is traversed by a straight line. Lattice points within a chosen window (gray-shaded strip) are orthogonally projected onto the line. If the line slope $\gamma = \tan\alpha$ is irrational, the projections (white circles) constitute a quasi-periodic 1-D sequence; otherwise, a periodic sequence is obtained.

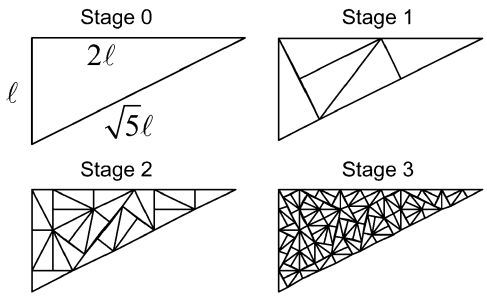

Fig. 3. Substitution rule for the *pinwheel* tiling (first three iterations).

[18]. Restrictions to prevent the creation of possible ordinary periodic or other uninteresting patterns, known as "matching rules," are enforced typically by edge-labeling-and-matching schemes (see Fig. 1), which can also be encoded in the tile shapes by means of small interlocking tabs on the edges, so as to allow only certain joinings [8], [18].

From among the many known categories of aperiodic tilings, we have found those referred to as *octagonal, Ammann, chair, table, sphinx, pinwheel, Danzer,* and *binary* [7], [8] promising for characterizing certain properties of our intended "tiled" antenna arrays (see Section IV). These categories, through various types and degrees of order and symmetry, provide a representative sampling of the realm of "orderly disorder."

1) Construction Rules and Algorithms: There are three principal procedures for constructing an aperiodic tiling: 1) by enforcing suitable local matching rules; 2) by projection techniques; and 3) by substitution processes. The first, and apparently most obvious, algorithmic approach consists of following jigsaw-puzzle rules, i.e., starting with a single tile and adding tiles according to local matching rules. However, this approach is not the most systematic and straightforward; since it involves alternative subjective (or random) choices at many stages, one will most likely reach a state where no additional "legal" matchings are possible (see, e.g., [19]).

A more systematic construction algorithm, applicable to categories of tilings such as *Penrose* and *octagonal,* is based on the "cut and project" method mentioned in Section II-A, which generates a *quasi-periodic* set via projection from a higher dimensional *periodic* lattice. This is illustrated for the simplest 1-D case in Fig. 2, where a 2-D square lattice is traversed by a straight line with given slope $\gamma = \tan\alpha$, and the lattice points within a given window are projected onto the line. If the line slope is *irrational,* these projections form a 1-D quasi-periodic sequence; otherwise, one obtains a periodic sequence. A particularly noteworthy case occurs when $\gamma = \tau = (1+\sqrt{5})/2$ (golden mean); now, one obtains a 1-D Fibonacci-type sequence (probably the most thoroughly studied 1-D aperiodic sequence) for which a number of rigorous results are available [17]. Generalization of the cut-and-project method to higher dimensions is straightforward. For instance, *Penrose* tilings like those in Fig. 1 can be obtained via projection of a five-dimensional periodic lattice onto a planar surface [19].

Another systematic procedure for constructing aperiodic tilings is the so-called "substitution method." This method can be applied to those categories of tilings having *hierarchial structure,* i.e., each tile can be decomposed into smaller copies of itself (and/or of the other tiles, if any). The substitution method employs decomposition of each tile, followed by a suitable rescaling (inflation) [8], [20]. An example of decomposition is illustrated in Fig. 3, in connection with the *pinwheel* tiling [8], [21]; the process is initiated with a right triangular tile with sides proportional to 1, 2, and $\sqrt{5}$, and the first three iterations are shown. This construction procedure, which can be iterated *ad infinitum* to tile the entire plane, resembles those utilized for the generation of certain classes of fractals. The *pinwheel* tiling in Fig. 3 displays much less evident order and symmetry than the *Penrose* tilings in Fig. 1 (see Section II-B.2 for more details).

The above construction algorithms are neither necessarily equivalent nor applicable for all categories of tilings. For instance, while *Penrose* tilings can be equivalently generated by any one of them, *pinwheel* tilings can only be generated via matching rules or substitution (not by projection) [12]. The reader is referred to [7], [8], [12], and [19] for more details.

2) Subtleties of Aperiodic Order: To understand the key properties of aperiodic tilings, the intuitive concepts of *order* and *symmetry,* which are traditionally tied to the concept of *periodicity,* need to be suitably extended. In aperiodic tilings, *order* can show up in diverse forms. A typical weak form of long-range order called *repetitiveness* is characterized by the occurrence of *any* bounded region of the whole tiling *infinitely often* across the tiling [8]. For *Penrose* tilings, a theorem by Conway [16] states that given any local pattern having a certain diameter, an identical pattern can be found within a distance of two diameters. Order is also manifested in the statistical frequency of occurrence of the individual tiles. Again, in *Penrose* tilings, the fractions of *kite* and *dart* tiles approach the golden mean $\tau = (1+\sqrt{5})/2$ for a plane-filling tiling; the same is true for the *thick* and *thin* rhombus tiles [16]. Different remnants of spatial order may also exist. For other categories of tilings (e.g., the *table, chair, Ammann* A4, and *sphinx* categories in Section IV), the vertices of the tiles form aperiodically defected 2-D rectangular or hexagonal lattices [7], [8]. Certain aperiodic tilings also exhibit some kind of *hierarchial structure,* i.e., the appearance of certain patterns at different scales (like fractals);

typical examples are provided by those categories of tilings generated by *substitution* processes (see Section II-B.1).

The other typical attribute of many aperiodic tilings is the presence of unusual *rotational* symmetries. *Penrose* tilings like those in Fig. 1 display arbitrarily large regions with centers of five-fold rotational symmetry [11]. This *local* property can be extended *globally* only in a *statistical* sense since every finite pattern of tiles can be shown to appear across the tiling in ten (and only ten) different rotational orientations, all with *the same* statistical frequency [11]; *Penrose* tilings are accordingly said to possess ten-fold rotational "statistical symmetry." Concerning the *pinwheel* tiling in Fig. 3, the visual impression of "less evident order and symmetry" is confirmed by the fact that *any* finite pattern appears across the tiling with *the same* statistical frequency in *all* rotational orientations [12], which means *full* rotational "statistical symmetry." The connections between statistical symmetry and spectral signatures of aperiodic tilings have been understood only recently [12] and will be touched in Section IV in connection with the antenna array radiation problem.

III. Applications Available in the Literature

As noted in Section I, Floquet theory provides the rigorous theoretical foundations for spectral-domain or spatial-domain analytic and numerical analysis of periodic structures. The Poisson summation formula [22] provides a systematic tool for recasting field observables as superpositions of either *individual* or *collective* contributions. Typical departures from perfect periodicity in realistic structures, such as truncation (finiteness) and weak perturbations in the spatial period as well as in the excitation (tapering), are addressed by methods like those in [23]–[25].

There is as yet *no* simple analog of Floquet theory for intrinsically aperiodic structures. For the seemingly simpler categories of quasi-periodic structures derived via cut-and-project methods (see Section II-B.1), periodicity can be *retrieved* by moving back to the *higher dimensional* generating lattice. However, particular care is needed, since intuitive attempts to generalize Floquet theory (from the higher dimensional periodic lattice to the lower dimensional quasi-periodic structure) may lead to erroneous conclusions (see, e.g., the discussion in [13]).

Recent investigations of photonic bandgap (PBG) quasi-crystals, in the form of 1-D aperiodically stacked multilayers and 2-D arrays of cylindrical rods placed at the vertices (or at the tile centers) of aperiodic tilings, have been reported in [26]–[35]. For the 1-D case, interesting results have been found for Fibonacci multilayers, revealing the self-similar fractal (Cantor-type) nature of the eigenspectra, and the presence of bandgaps and *critical* localization phenomena (see, e.g., [27] and the references therein). For the 2-D case, results are available for PBG quasi-crystals with five-fold *(Penrose)* [30], [32]–[34], eight-fold, [26], [34], ten-fold [28], and 12-fold [29], [31] symmetry, as well as for Fibonacci-type [35]. The most interesting observations can be summarized as follows.

i) Periodicity does not seem to be essential to obtaining complete bandgaps.

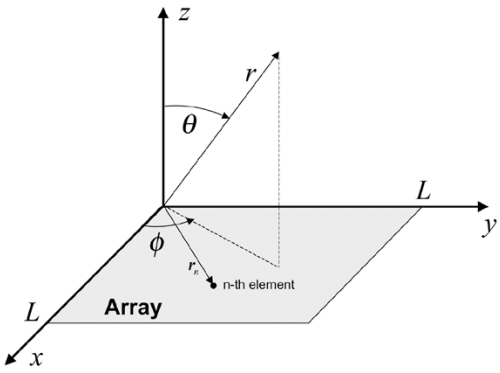

Fig. 4. Problem geometry for the antenna array configuration, with relevant Cartesian (x, y, x) and spherical (r, θ, ϕ) coordinate systems. Antenna elements are arranged in the (x, y) plane at the vertices $\mathbf{r}_n \equiv (x_n, y_n)$ of a square patch (side L) of a given aperiodic tiling.

ii) Bandgaps in PBG quasi-crystals are mainly governed by the *short-range* environment, and are remarkably *almost independent* of the incidence angle.

iii) PBG quasi-crystals seem to offer additional degrees of freedom in the creation of localized defect modes.

Against this background, as noted in Section I, we have initiated our study of a new problem category: radiation from aperiodic-tiling antenna arrays.

IV. Aperiodic-Tiling Antenna Arrays

Use of *aperiodic* geometries is a well-known device to achieve *array thinning* (i.e., mean interelement spacing greater than half a wavelength), avoiding at the same time the appearance of *grating lobes* (and the related scanning limitations) [36], [37]. In a broader setting, not necessarily limited to array thinning, use of *fractal* geometries has also proved to be advantageous (see [4] and [38]–[40]). Here, we shall explore how these and other features show up in aperiodic-tiling arrays.

A. Array Geometry

The problem geometry is depicted in Fig. 4, with the relevant Cartesian (x, y, z) and spherical (r, θ, ϕ) coordinate systems. A planar array in the (x, y) plane is considered, with identical antenna elements placed at the vertices of a square patch (side L) of a given aperiodic tiling; the generic nth element position is denoted by $\mathbf{r}_n \equiv (x_n, y_n)$. Our interest lies in the study of the radiation properties of this structure, for time-harmonic excitation with implicit $\exp(j\omega t)$ dependence. The ensuing analysis is also intimately related to the problem of plane wave scattering from (transmission through) planar arrays of electrically small obstacles (holes). We assume uniform excitation with negligible interelement coupling. For observation distance r in the Fraunhofer region, $r \gg 2L^2/\lambda$, with $\lambda = 2\pi c/\omega$ denoting the ambient wavelength ($c = 1/\sqrt{\epsilon\mu}$ being the ambient wavespeed), the array is characterized by the "array factor" [36]

$$\begin{aligned} F_s(u,v) &= \sum_{n=1}^{N} \exp[j2\pi(ux_n + vy_n)] \\ &= \sum_{n=1}^{N} \exp[jk\sin\theta(x_n\cos\phi + y_n\sin\phi)] \\ &= F_p(\theta,\phi) \end{aligned} \tag{4}$$

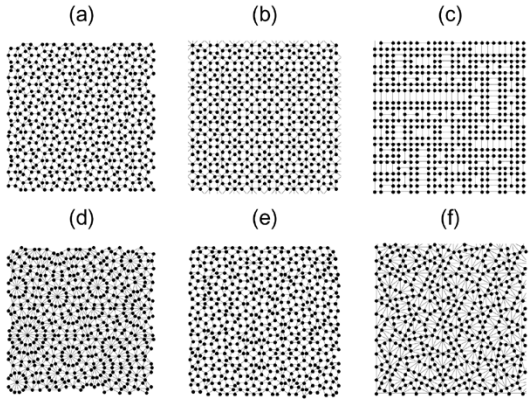

Fig. 5. Array antenna configurations obtained from square patches (of side L) of six representative categories of aperiodic tilings. Tiling geometries are sketched in background with light lines, and antenna element positions are marked with black dots. (a) *Penrose thick-and-thin* ($N = 530, d_{\rm av} = 0.818d_0, d_{\rm min} = 0.613d_0, d_{\rm max} = 1.075d_0$); (b) *octagonal* ($N = 532, d_{\rm av} = 0.898d_0, d_{\rm min} = 0.834d_0, d_{\rm max} = 1.089d_0$); (c) *table* ($N = 538, d_{\rm av} = d_{\rm min} = d_{\rm max} = 0.88d_0$); (d) *Danzer* ($N = 529, d_{\rm av} = 0.697d_0, d_{\rm min} = 0.64d_0, d_{\rm max} = 1.438d_0$); (e) *binary* ($N = 534, d_{\rm av} = 0.855d_0, d_{\rm min} = 0.662d_0, d_{\rm max} = 1.073d_0$); (f) *pinwheel* ($N = 532, d_{\rm av} = 0.8d_0, d_{\rm min} = 0.726d_0, d_{\rm max} = 1.148d_0$). The reference interelement spacing d_0 pertains to a square periodic 23×23 element array of side L.

where $k = 2\pi/\lambda$ is the ambient wavenumber and $u = \lambda^{-1}\sin\theta\cos\phi$ and $v = \lambda^{-1}\sin\theta\sin\phi$ denote the wavenumber-spectral variables in the x and y directions, respectively.

From a comprehensive parametric analysis of the radiation properties of many categories of aperiodic-tiling antenna arrays, we have selected six representative geometries. The corresponding prototype arrays are illustrated in Fig. 5. Besides the already introduced *Penrose thick-and-thin* [Fig. 5(a)] and *pinwheel* [Fig. 5(f)] tilings, we have the so-called *octagonal* (Ammann-Beenker) [Fig. 5(b)], *table* [Fig. 5(c)], *Danzer* [Fig. 5(d)], and *binary* [Fig. 5(e)] geometries [7], [8], [20]. The corresponding tilings have been generated via Mathematica [41] implementing the algorithms in [7], [8], and [19]; the reader is referred to [42] for alternative software tools. Specifically, the *Penrose thick-and-thin* and the *octagonal* tilings have been generated via projection methods (see Section II-B.1) [19]. The remaining tilings have been generated via substitution processes (see Section II-B.1) [7], [8]. The basic substitution rules to be iterated are shown in Fig. 6, with the exception of those pertaining to the *pinwheel* tiling already shown in Fig. 3. From a given tiling, the corresponding array has been obtained by considering the tile vertices within a square patch, with size and scaling suitably chosen so as to maintain the number of elements approximately the same ($N \approx 530$), the benchmark configuration being a square periodic array of 23×23 elements. Also indicated in the caption of Fig. 5 are the average, minimum, and maximum values ($d_{\rm av}, d_{\rm min}, d_{\rm max}$, respectively) of the nearest neighborhood spacing for each array

$$d_n = \min_{m \neq n} |\mathbf{r}_n - \mathbf{r}_m|, \quad n = 1, \ldots, N. \tag{5}$$

In order to facilitate meaningful comparison among N-element arrays of the same electrical size (and, hence, comparable beamwidth), it is expedient to normalize dimensional quantities with respect to suitable reference values pertaining to

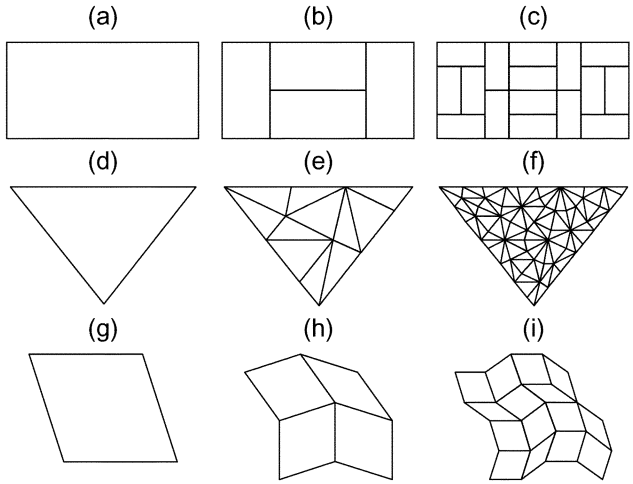

Fig. 6. Initial stage and first two iterations for the tiling geometries in Fig. 5 generated via substitution. (a), (b), (c) *Table*; (d), (e), (f) *Danzer*; (g), (h), (i) *binary*. For the *pinwheel* tiling, see Fig. 3.

an equivalent N-element square periodic array. We utilize, in particular, the reference periodic interelement spacing d_0 and corresponding frequency f_0 relative to a uniform $\lambda/2$ interelement spacing

$$d_0 = L/\sqrt{N-1}, \quad f_0 = c/(2d_0). \tag{6}$$

Although not unambiguously discernible in Fig. 5, the chosen categories of tilings are representative of various types and degrees of order and symmetry. Specifically, as already mentioned in Section II-B.2, the *Penrose* and *pinwheel* tilings exhibit tenfold and *full* statistical symmetry, respectively [8]. The *octagonal, Danzer,* and *binary* tilings exhibit statistical symmetries of order 8, 14, and 10, respectively [8]. Moreover, the *Penrose, octagonal,* and *table* tilings are *more orderly* than the *Danzer, binary,* and *pinwheel* tilings. In particular, *Penrose* and *octagonal* tilings are quasi-periodic (in the terminology of Section II-A), whereas the *table* tiling is readily identified as an aperiodically defected square lattice [see Fig. 5(c)]. Conversely, *Danzer, binary,* and *pinwheel* tilings are somehow more *random-looking*. It should also be pointed out that the spectral properties of these categories of tilings have been studied and characterized within the framework of crystallography (see, e.g., [8], [13], and [43]). Relevant results will be exploited for phenomenological interpretation, capitalizing on the formal equivalence between the array factor in (4) and the X-ray diffraction spectrum.

B. Results

1) Radiation Spectra: The radiation spectra $|F_s(u,v)|^2$ of the arrays in Fig. 5 are shown in Fig. 7. It is well-known that the radiation spectra of *periodic* arrays are characterized by *discrete* (Floquet) wavenumber components [36], whereas for *random* arrays, they are dominated by *continuous* features. One would therefore expect that the radiation spectra of aperiodic-tiling arrays contain in general both *discrete* (highly localized) and *continuous* (diffused) constituents (see Section IV-C), depending on the degree of *long-range order*. From visual inspection of Fig. 7, the presence of sharp peaks is particularly evident for the *Penrose* tiling [Fig. 7(a)], the *octagonal* tiling [Fig. 7(b)], and the *table* tiling [Fig. 7(c)] arrays (using known results from

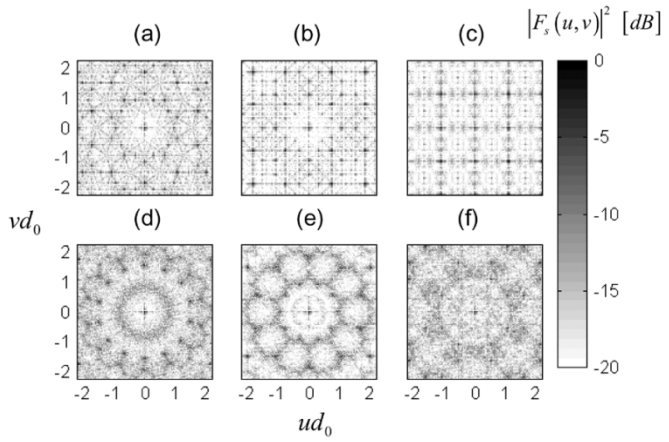

Fig. 7. Radiation spectra $|F_s(u,v)|^2$ in (4) pertaining to the arrays in Fig. 5. (a) *Penrose* thick-and-thin; (b) *octagonal*; (c) *table*; (d): *Danzer*; (e) *binary*; (f) *pinwheel*.

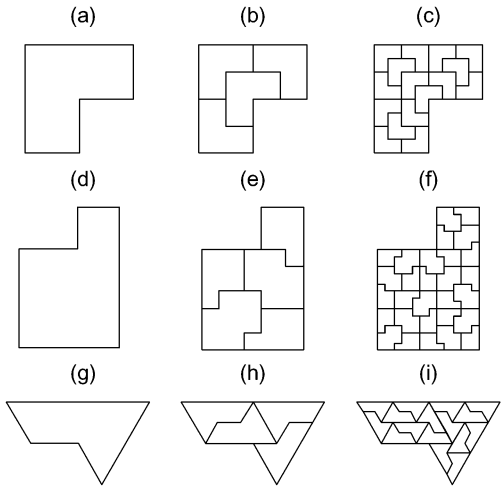

Fig. 8. Initial stage and first two iterations for representative categories of aperiodic tilings amenable to aperiodically defected lattices. (a), (b), (c) *Chair*; (d), (e), (f) *Ammann A4*; (g), (h), (i) *sphinx*. Radiation characteristics of antenna arrays based on these geometries are not reported for brevity (see the discussion in Section IV-B).

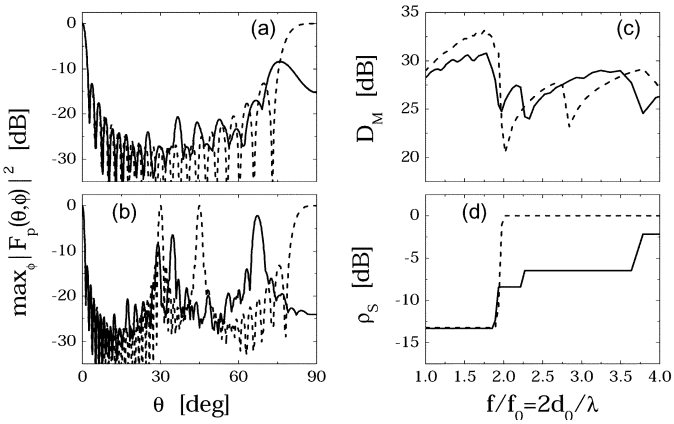

Fig. 9. *Penrose* tiling array as in Fig. 5(a). (a), (b) Radiation pattern maximum (with respect to azimuthal angle ϕ) versus elevation angle θ at frequency $f = 2f_0 (d_0 = \lambda, d_{\rm av} = 0.818\lambda, d_{\min} = 0.613\lambda, d_{\max} = 1.075\lambda)$ and $f = 4f_0 (d_0 = 2\lambda, d_{\rm av} = 1.635\lambda, d_{\min} = 1.226\lambda, d_{\max} = 2.151\lambda)$, respectively. (c), (d) Maximum directivity D_M in (7) and sidelobe ratio ρ_S in (8), respectively, versus scaled frequency $f/f_0 = 2d_0/\lambda$. The frequency f_0 corresponds to $d_0 = \lambda/2$ uniform interelement spacing for a square periodic 23×23 element array, whose reference behavior is displayed as dashed curves.

crystallography [8], [13], [43], it can actually be shown that, in the infinite-size limit, the radiation spectra of these arrays are discretized, and that the discrete footprints become diffused under spatially truncated conditions). Specifically, the *Penrose* and *octagonal* tilings have *purely discrete* spectra, whereas the *table* tiling is characterized by a *mixed* (discrete/continuous) more diffused spectrum [8], [13], [43]. The high-intensity dark spots in the radiation spectra pertaining to these three categories should thus be viewed as the analog of grating lobes for periodic arrays. Conversely, the radiation spectra of the *Danzer, binary,* and *pinwheel* tiling arrays [Figs. 7(d), (e), and (f), respectively] are more diffused since it can be shown that the radiation spectra of these arrays are *continuous* in the infinite-size limit [8], [13], [43]; these array geometries *do not* possess features analogous to grating lobes.

Another striking feature of the radiation spectra in Fig. 7 is their high degree of *symmetry*, in spite of the fact that *none* of the array geometries in Fig. 5 is either perfectly symmetric or periodic. Such spectral signatures reflect the *statistical* symmetry properties of the corresponding tilings (see also Section IV-C). In particular, the radiation spectra of the *Penrose* tiling [Fig. 7(a)] and *octagonal* tiling [Fig. 7(b)] arrays exhibit ten-fold and eight-fold symmetry, respectively. Similar (ten-fold symmetric) qualitative behavior was observed for the kite-and-dart version of the *Penrose* tiling. The radiation spectrum of the *table*-tiling array [Fig. 7(c)] is not very different from that of a regular periodic square array, with grating lobes at $u, v = m/d_0, m = \pm 1, \pm 2, \ldots$. We have also studied the radiation properties of other categories of aperiodic tilings that can be parameterized on aperiodically defected lattices. Fig. 8 shows three representative examples known as *chair, Ammann A4,* and *sphinx* [7], [8]. At variance with the *table* tiling, the radiation spectra of these tilings are *known* to be *purely discrete* [8], [13], [43]. However, their radiation properties (not shown here for brevity) were found not to exhibit particularly interesting differences from those pertaining to the corresponding periodic lattices (rectangular for *chair* and *Ammann A4,* and hexagonal for *sphinx*). Completing the inspection of Fig. 7, the radiation spectra of the *Danzer* tiling [Fig. 7(d)] and of the *binary* tiling [Fig. 7(e)] arrays exhibit 14-fold and ten-fold symmetry, respectively, whereas the radiation spectrum of the *pinwheel* tiling [Fig. 7(f)] looks more isotropic.

2) Array-Oriented Observables: In order to explore the potential utility of the above characteristics in practical applications for each of the array configurations, we have displayed typical quantities of interest in Figs. 9–14. Spatial and frequency quantities are scaled to reference values (d_0, f_0) pertaining to a square periodic 23×23 element array. Each figure contains two representative cuts [labeled (a) and (b)] of the radiation patterns at frequencies $f = 2f_0$ and $f = 4f_0$, corresponding to equivalent periodic interelement spacings $d_0 = \lambda$ and $d_0 = 2\lambda$, respectively. As a compact measure of both the beamwidth and the (worst case) sidelobe level characteristics, the quantity displayed in these two diagrams is the maximum (over the azimuthal angle ϕ) of the radiation pattern $|F_p(\theta,\phi)|^2$. Also dis-

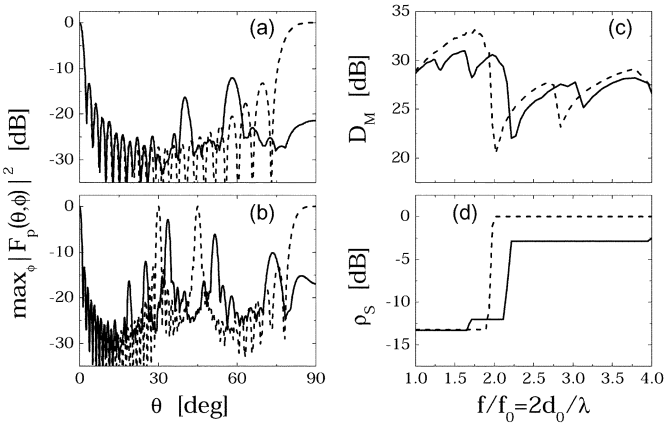

Fig. 10. As in Fig. 9, but for the *octagonal* tiling array in Fig. 5(b). Interelement spacing in (a) and (b) is $(d_{\rm av} = 0.898\lambda, d_{\min} = 0.834\lambda, d_{\max} = 1.089\lambda)$ and $(d_{\rm av} = 1.796\lambda, d_{\min} = 1.668\lambda, d_{\max} = 2.179\lambda)$, respectively.

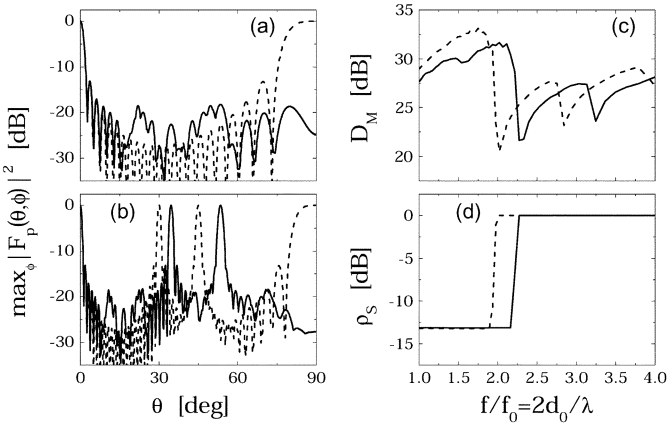

Fig. 11. As in Fig. 9, but for the *table* tiling array in Fig. 5(c). Interelement spacing in (a) and (b) is $(d_{\rm av} = d_{\min} = d_{\max} = 0.88\lambda)$ and $(d_{\rm av} = d_{\min} = d_{\max} = 1.76\lambda)$, respectively.

played, as a function of frequency, are the array maximum directivity [labeled (c)]

$$D_M = \frac{4\pi \max_{\theta,\phi} |F_p(\theta,\phi)|^2}{\int_0^\pi d\theta \int_0^{2\pi} d\phi |F_p(\theta,\phi)|^2 \sin\theta} \tag{7}$$

and the sidelobe ratio (SLR) [labeled (d)]

$$\rho_S = \frac{\max_{(\theta,\phi)\notin\mathcal{B}} |F_p(\theta,\phi)|^2}{\max_{\theta,\phi} |F_p(\theta,\phi)|^2} \tag{8}$$

with $\mathcal{B}$ denoting the main lobe angular region. In each plot, the dashed curves depict the reference behavior of the 23×23 square periodic array. From this reference behavior, one observes the well-known appearance of the first grating lobe (with the same amplitude as the main lobe) at frequency $f = 2f_0$ (i.e., $d_0 = \lambda$ interelement spacing), with the corresponding step increase of the SLR. The frequency behavior of the directivity is consequently characterized by a broad dynamic range, with abrupt variations corresponding to the appearance (in the visible range) of grating lobes, and an overall min-to-max variation of about 15 dB.

For the *Penrose* tiling, *octagonal* tiling, and *table* tiling arrays, characterized by the presence of *discrete* spectral constituents, one would not expect large deviations from the reference behavior. This is especially true for the *table* tiling

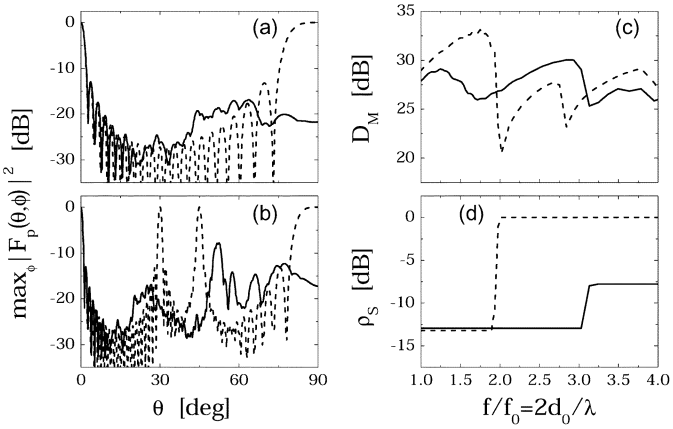

Fig. 12. As in Fig. 9, but for the *Danzer* tiling array in Fig. 5(d). Interelement spacing in (a) and (b) is $(d_{\rm av} = 0.697\lambda, d_{\min} = 0.64\lambda, d_{\max} = 1.438\lambda)$ and $(d_{\rm av} = 1.393\lambda, d_{\min} = 1.279\lambda, d_{\max} = 2.877\lambda)$, respectively.

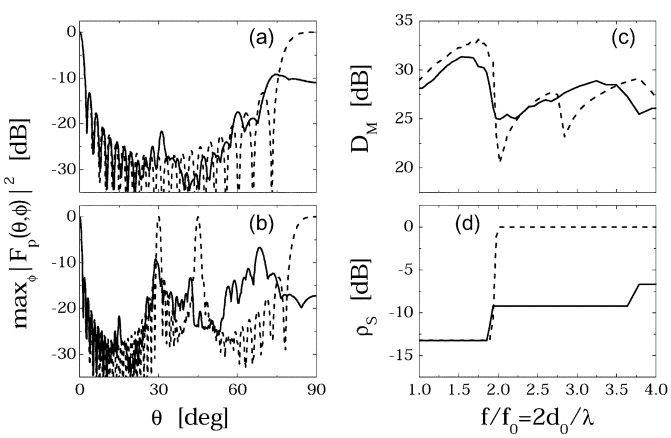

Fig. 13. As in Fig. 9, but for the *binary* tiling array in Fig. 5(e). Interelement spacing in (a) and (b) is $(d_{\rm av} = 0.855\lambda, d_{\min} = 0.662\lambda, d_{\max} = 1.073\lambda)$ and $(d_{\rm av} = 1.711\lambda, d_{\min} = 1.324\lambda, d_{\max} = 2.147\lambda)$, respectively.

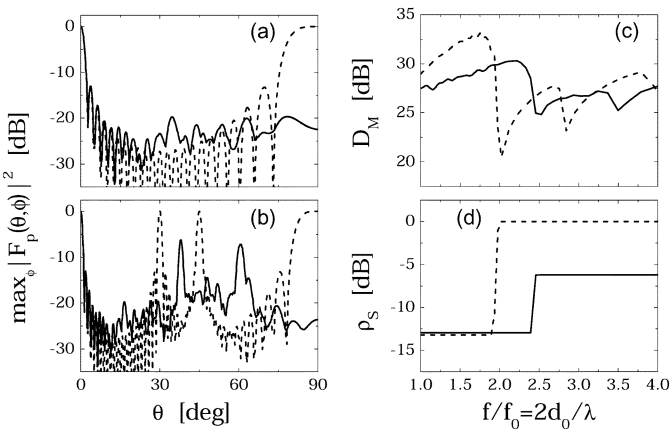

Fig. 14. As in Fig. 9, but for the *pinwheel* tiling array in Fig. 5(f). Interelement spacing in (a) and (b) is $(d_{\rm av} = 0.8\lambda, d_{\min} = 0.726\lambda, d_{\max} = 1.148\lambda)$ and $(d_{\rm av} = 1.6\lambda, d_{\min} = 1.452\lambda, d_{\max} = 2.296\lambda)$, respectively.

array (Fig. 11), where one essentially observes a slight positive shift $(\sim 0.25 f_0)$ in frequency and the consequent disappearing of grating lobes at $f = 2f_0$ [i.e., equivalent periodic interelement spacing $d_0 = \lambda$; see Fig. 11(a)]. For the *Penrose* tiling (Fig. 9) and *octagonal* tiling (Fig. 10) arrays, the behavior is

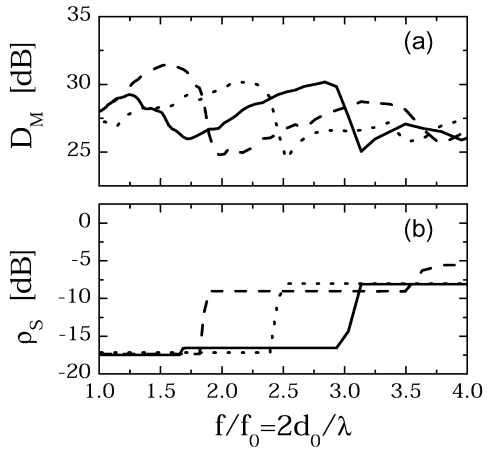

Fig. 15. As in Figs. 12–14(c) and (d), but for *circular* patches with same area. — *Danzer* tiling array ($N = 530$); - - - *binary* tiling array ($N = 528$); · · · · · · *pinwheel* tiling array ($N = 524$).

slightly different. Grating lobes are still visible, but their amplitude is smaller than the main lobe, with a consequent moderate reduction in dynamic range for the directivity and SLR.

Considerably different behaviors are observed for the *Danzer* tiling, *binary* tiling, and *pinwheel* tiling arrays, for which the predominance of continuous spectral components yields lower SLR values over fairly broad frequency ranges. In particular, the *Danzer* tiling array (Fig. 12) exhibits SLR values comparable to the best performance achievable with a periodic square array (~ -13 dB), but over a considerably broader frequency band (up to nearly $f = 3f_0$, i.e., equivalent periodic interelement spacing $d_0 = 1.5\lambda$). For the *pinwheel* tiling array (Fig. 14), similar SLR values are achieved up to nearly $f = 2.5f_0$ (i.e., equivalent periodic interelement spacing $d_0 = 1.25\lambda$). The *binary*-tiling array (Fig. 13) exhibits slightly larger SLR values (~ -10 dB), but over a broader frequency band (up to nearly $f = 3.5f_0$, i.e., equivalent periodic interelement spacing $d_0 = 1.75\lambda$). We verified that the minimum SLR values (~ -13 dB) achievable with these three types of arrays are essentially related to the array boundary shape (approximately square in the above simulations). Fig. 15 shows the maximum directivity and the SLR for arrays with *circular* boundaries in these three types of tilings, preserving the same area and comparable number of elements as in the square-array simulations above. One observes the same qualitative behavior as in Figs. 12–14(c) and (d), but with minimum SLR values of about -17 dB. For these three categories of tilings, the maximum SLR values were found to decrease slowly with increasing array size, for both square and circular boundaries.

C. Remarks

A few remarks are in order, concerning the effects of *order* and *symmetry* in the radiation properties and their potential applications. The examples presented in Section IV-B indicate that the type and degree of order and symmetry, which characterize a tiling, leave distinct footprints in the radiation spectrum. Note that the seemingly *ambiguous* connection between tilings (i.e., collections of polygons) and point sets (in our context, antenna element positions) can be established rigorously using standard tools of discrete geometry [13], [43]. Here, we merely highlight that the salient *qualitative* features of the EM response are independent of precisely how antenna elements are configured for each type of tiles, provided that no accidental symmetries are introduced by this process [12]. We also verified that results in Figs. 7 and 9–15 depend *only weakly* on the position of the chosen subset of boundary-determining vertices across the tiling.

Summarizing the observations in Section IV-B, the interplay between discrete and continuous constituents in the radiation spectrum depends on the degree of long-range order in the array geometry. The reader is referred to [8], [13], and [43] for theoretical details. Consequently, strong collective interference phenomena (grating lobes) are clearly visible for the more orderly appearing tilings *(Penrose, octagonal, table)* and tend to be smoothed out for the more random-appearing tilings (Danzer, *binary*, *pinwheel*). More in general, quasi-periodic tilings (e.g., those generated by projection) have discrete spectra, whereas tilings generated via substitution may exhibit either discrete or continuous spectra depending on the eigenvalues of the linear transformation matrix which implements the substitution rule (see [8], [13], [43] for details).

The connection between the spatial symmetry properties of aperiodic tilings and their spectral properties has been established only recently (see, e.g., [12]). It can been shown that the radiation spectrum is sensitive primarily to the *statistical* symmetry of the tiling. This notion of symmetry is a generalization (weakening) of the intuitive concept, where one shifts the focus from the tiling itself to the relationship between its parts (tiles). The statistical symmetry of interest here concerns the rotational invariance of the statistical frequencies of occurrence of the various tiles (or sets of them) in the same orientation, which manifests itself in the wave-dynamical radiation spectra (cf. Fig. 7) through a corresponding overall symmetry.

To assess the effects of long-range order and statistical symmetry, it is instructive to compare the radiation spectra of the Penrose-tiling [Fig. 7(a)] and the *binary*-tiling [Fig. 7(e)] arrays. These two tilings are constructed using the same set of tiles (thick and thin rhombuses, with the same statistical occurrence) and they both exhibit 10-fold statistical symmetry. However, the Penrose tiling is quasi-periodic (and thus possesses long-range order), whereas the *binary* tiling is more random-like. Consequently, both radiation spectra exhibit 10-fold rotational symmetry, but the Penrose-tiling spectrum looks more *discrete* whereas the *binary*-tiling spectrum looks more *continuous*. The *pinwheel* tiling represents another interesting paradigm, since its radiation spectrum [Fig. 7(f)] is essentially continuous and fully rotationally invariant, and would therefore seem undistinguishable from the spectrum of a random array. However, as discussed in [12], its deterministic nature shows up in some *self-similar* features of the spectrum. These features reflect the hierarchial symmetry typical of tilings generated by substitution (see Section II-B.2).

V. Conclusion

The radiation properties of planar antenna arrays based on certain representative categories of aperiodic tilings have been

analyzed and discussed, after presentation and review of background material on aperiodic tilings as well as known results concerning their EM properties. Representative displays from a comprehensive comparative parametric analysis have illustrated the effects of *weak* forms of order and symmetry in the radiation properties of selected tiling geometries. Concerning potential applications, certain of the array geometries (Danzer, *binary*, *pinwheel* tilings) considered in our preliminary investigation here seem to give rise to interesting *broadband* performance in terms of sidelobe level. In this connection, further investigation of circuit characteristics (input impedance, feeding network, etc.) as well as polarization properties would be necessary to come up with potentially useful design rules. Other worthwhile issues are concerned with the study of the array "robustness" with respect to possible antenna element failure or misplacement. Exploration of other categories of aperiodic tilings (e.g., Fibonacci) is also suggestive. Studies pertaining to the scattering (transmission) properties of aperiodic-tiling arrays of obstacles (apertures) are already in progress. It is hoped that this agenda may eventually provide new perspectives for the synthesis of broadband and multi-beam antenna arrays, and artificial surfaces with peculiar spectral signatures.

ACKNOWLEDGMENT

The authors would like to express their appreciation to Prof. L. Danzer (University of Dortmund, Germany) and Dr. Z. Papadopolos (University of Tübingen, Germany) for valuable suggestions.

REFERENCES

[1] R. W. Ziolkowski and N. Engheta, Eds., *IEEE Trans. Antennas Propag. Special Issue on Metamaterials*, Oct., pt. I, vol. 51, no. 10, 2003.

[2] P.-S. Kildal, A. Kishk, and S. Maci, Eds., *IEEE Trans. Antennas Propag. Special Issue on Artificial Magnetic Conductors, Soft/Hard Surfaces, and Other Complex Surfaces*, Jan., pt. I, vol. 53, no. 1, 2005.

[3] D. L. Jaggard, "Fractal electrodynamics: Wave interactions with discretely self-similar structures," in *Symmetry in Electromagnetics*, C. Baum and H. Kritikos, Eds. Washington, DC: Taylor and Francis Publishers, 1995, pp. 231–280.

[4] D. H. Werner and R. Mittra, Eds., *Frontiers in Electromagnetics*. Piscataway, NJ: IEEE Press, 2000.

[5] D. Shechtman, I. Blech, D. Gratias, and J. W. Cahn, "Metallic phase with long-range orientational order and no translation symmetry," *Phys. Rev. Letts.*, vol. 53, no. 20, pp. 1951–1953, Nov. 1984.

[6] D. Levine and P. J. Steinhardt, "Quasicrystals: A new class of ordered structures," *Phys. Rev. Letts.*, vol. 53, no. 26, pp. 2477–2480, Dec. 1984.

[7] B. Grünbaum and G. C. Shepard, *Tilings and Patterns*. New York: Freeman, 1987.

[8] M. Senechal, *Quasicrystals and Geometry*, Cambridge, U.K.: Cambridge Univ. Press, 1995.

[9] R. Lifshitz, "Quasicrystals: A matter of definition," *Found. Phys.*, vol. 33, no. 12, pp. 1703–1711, Dec. 2003.

[10] C. Corduneanu, *Almost Periodic Functions*, 2nd ed. New York: Chelsea, 1989.

[11] C. Radin, *Miles of Tiles*. Providence, RI: American Mathematical Society, 1999.

[12] ——, "Symmetries of quasicrystals," *J. Stat. Phys.*, vol. 95, no. 5/6, pp. 827–833, 1999.

[13] M. Baake, "A guide to mathematical quasicrystals," in *Quasicrystals: An Introduction to Structure, Physical Properties, and Applications*, J.-B. Suck, M. Schreiber, and P. Häussler, Eds, Berlin, Germany: Springer, 2002, pp. 17–48.

[14] H. Wang, "Proving theorems by pattern recognition," *Bell Syst. Tech. J.*, vol. 40, pp. 1–41, 1961.

[15] R. Berger, "The undecidability of the domino problem," *Mem. Amer. Math. Soc.*, vol. 66, pp. 1–72, 1966.

[16] R. Penrose, "The rôle of aesthetics in pure and applied mathematical research," *Bull. Inst. Math. Appl.*, vol. 10, pp. 266–271, 1974.

[17] S. Vajda, *Fibonacci and Lucas Numbers, and the Golden Section: Theory and Applications*. New York: Halsted Press, 1989.

[18] M. Gardner, "Extraordinary nonperiodic tiling that enriches the theory of tiles," *Sci. Amer.*, vol. 236, pp. 110–119, Dec. 1977.

[19] U. Grimm and M. Schreiber, "Aperiodic tilings on the computer," in *Quasicrystals: An Introduction to Structure, Physical Properties, and Applications*, J.-B. Suck, M. Schreiber, and P. Häussler, Eds, Berlin, Germany: Springer, 2002, pp. 49–66.

[20] K.-P. Nischke and L. Danzer, "A construction of inflation rules based on n-fold symmetry," *Discrete Comput. Geom.*, vol. 15, no. 2, pp. 221–236, Feb. 1996.

[21] C. Radin, "The pinwheel tilings of the plane," *Ann. Math.*, vol. 139, pp. 661–702, 1994.

[22] A. Papoulis, *The Fourier Integral and Its Applications*. New York: McGraw-Hill, 1962.

[23] L. Carin and L. B. Felsen, "Time-harmonic and transient scattering by finite periodic flat strip arrays: Hybrid (ray)-(Floquet mode)-(MOM) algorithm and its GTD interpretation," *IEEE Trans. Antennas Propagat.*, vol. 41, no. 4, pp. 412–421, Apr. 1993.

[24] L. B. Felsen and L. Carin, "Diffraction theory and of frequency- and time-domain scattering by weakly aperiodic truncated thin-wire gratings," *J. Opt. Soc. Amer. A*, vol. 11, no. 4, pp. 1291–1306, Apr. 1994.

[25] A. Cucini, M. Albani, and S. Maci, "Truncated Floquet wave full-wave analysis of large phased arrays of open-ended waveguides with a nonuniform amplitude excitation," *IEEE Trans. Antennas Propag.*, vol. 51, no. 6, pp. 1386–1394, Jun. 2003.

[26] Y. S. Chan, C. T. Chan, and Z. Y. Liu, "Photonic band gaps in two dimensional photonic quasicrystals," *Phys. Rev. Letts.*, vol. 80, no. 5, pp. 956–959, Feb. 1998.

[27] E. Maciá, "Optical engineering with Fibonacci dielectric multilayers," *Appl. Phys. Letts.*, vol. 73, no. 23, pp. 3330–3332, Dec. 1998.

[28] C. Jin, B. Cheng, B. Man, Z. Li, D. Zhang, S. Ban, and D. Sun, "Band gap and wave guiding effect in a quasiperiodic photonic crystal," *Appl. Phys. Letts.*, vol. 75, no. 13, pp. 1848–1850, Sept. 1999.

[29] C. Jin, B. Cheng, B. Man, Z. Li, and D. Zhang, "Two-dimensional dodecagonal and decagonal quasiperiodic photonic crystals in the microwave region," *Phys. Rev. B*, vol. 61, no. 16, pp. 10 762–10 767, Apr. 2000.

[30] M. A. Kaliteevski, S. Brand, R. A. Abram, T. F. Krauss, R. M. De La Rue, and P. Millar, "Two-dimensional penrose-tiled photonic quasicrystals: Diffraction of light and fractal density of modes," *J. Mod. Opt.*, vol. 47, no. 11, pp. 1771–1778, Nov. 2000.

[31] X. Zhang, Z.-Q. Zhang, and C. T. Chan, "Absolute photonic band gaps in 12-fold symmetric photonic quasicrystals," *Phys. Rev. B*, vol. 63, 2001. 081 105(R).

[32] M. Bayndir, E. Cubukcu, I. Bulu, and E. Ozbay, "Photonic band-gap effect, localization, and waveguiding in the two-dimensional penrose lattice," *Phys. Rev. B*, vol. 63, 2001. 161 104(R).

[33] ——, "Photonic band gaps and localization in two-dimensional metallic quasicrystals," *Europhys. Letts.*, vol. 56, no. 1, pp. 41–46, Oct. 2001.

[34] M. Hase, H. Miyazaki, M. Egashira, N. Shinya, K. M. Kojima, and S. Uchida, "Isotropic photonic band gap and anisotropic structures in transmission spectra of two-dimensional fivefold and eightfold symmetric quasiperiodic photonic crystals," *Phys. Rev. B*, vol. 66, 2002. 214 205.

[35] Z. Ouyang, C. Jin, D. Zhang, B. Cheng, X. Meng, G. Yang, and J. Li, "Photonic bandgaps in two-dimensional short-range periodic structures," *J. Opt. A: Pure Appl. Opt.*, vol. 4, no. 1, pp. 23–28, Jan. 2002.

[36] *Phased Array Antenna Handbook*, Artech House, Boston, MA, 1994. R. J. Mailloux.

[37] B. D. Steinberg, "Comparison between the peak sidelobe of the random array and algorithmically designed aperiodic arrays," *IEEE Trans. Antennas Propagat.*, vol. 21, no. 3, pp. 366–370, May 1973.

[38] Y. Kim and D. L. Jaggard, "The fractal random array," *Proc. IEEE*, vol. 74, no. 9, pp. 1278–1280, Sept. 1986.

[39] C. Puente-Baliarda and R. Pous, "Fractal design of multiband and low side-lobe arrays," *IEEE Trans. Antennas Propag.*, vol. 44, no. 5, pp. 730–739, May 1996.

[40] D. H. Werner, W. Kuhirun, and P. L. Werner, "The Peano-Gosper fractal array," *IEEE Trans. Antennas Propag.*, vol. 51, no. 8, pp. 2063–2072, Aug. 2003.

[41] R. Maeder, *Programming in Mathematica*. Redwood City, CA: Addison-Wesley, 1990.

[42] [Online]. Available: www.geom.uiuc.edu/software/tilings/TilingSoftware.html

[43] B. Solomyak, "Spectrum of a dynamical system arising from Delone sets," in *Quasicrystals and Discrete Geometry*, J. Patera, Ed. Providence, RI: Fields Institute Monographs, American Mathematical Society, 1998, vol. 10, pp. 265–275.

Vincenzo Pierro was born in Salerno, Italy, in 1967. He received the Laurea degree (*summa cum laude*) in physics from the University of Salerno, Italy, in 1990.

In 1991, he held a visiting position in the COLUMBUS Metrology Group at the European Space Research & Technology Centre (ESTEC-ESA), Noordwijk, The Netherlands. Since 1996, he has been with the Faculty of Engineering, University of Sannio, Benevento, Italy, where he was appointed Assistant Professor of Electromagnetics in 1996, and Associate Professor in 2001. His main research interests are in the field of complex electromagnetic systems, electromagnetic detection of gravitational waves, and applied mathematics.

Dr. Pierro is a Member of the Italian Physical Society (SIF). He was awarded a research fellowship in 1999 from the Japan Society for the Promotion of Science (JSPS), in connection with the TAMA 300 experiment.

Vincenzo Galdi (M'98–SM'04) was born in Salerno, Italy, on July 28, 1970. He received the Laurea degree (*summa cum laude*) in electrical engineering and the Ph.D. degree in applied electromagnetics from the University of Salerno, Italy, in 1995 and 1999, respectively.

From April to December 1997, he held a visiting position in the Radio Frequency Division of the European Space Research & Technology Centre (ESTEC-ESA), Noordwijk, The Netherlands. From September 1999 to August 2002, he held a Research Associate position in the Department of Electrical and Computer Engineering at Boston University, Boston, MA. In November 2002, he was appointed Associate Professor of Electromagnetics, and joined the Department of Engineering at the University of Sannio, Benevento, Italy, where he is currently working. His research interests include analytical and numerical techniques for wave propagation in complex environments, electromagnetic chaos, and inverse scattering.

Dr. Galdi is a Member of Sigma Xi. He is the recipient of a 2001 International Union of Radio Science (URSI) "Young Scientist Award."

Giuseppe Castaldi was born in Benevento, Italy, in 1968. He received the Laurea degree (*summa cum laude*) in electrical engineering from the "Federico II" University of Naples, Italy, in 1995, and the Ph.D. degree in applied electromagnetics from the University of Salerno, Italy, in 1999.

In 2001, he was a Postdoctoral Research Fellow at the TNO Physics and Electronics Laboratory, The Hague, The Netherlands. In 2003, he was appointed Assistant Professor of Electromagnetics and joined the Department of Engineering at the University of Sannio, Benevento, where he is currently working. His research interests include electromagnetic chaos, quasi-periodic antenna arrays, applications of neural networks to inverse scattering problems, and field representations in complex environments.

Innocenzo M. Pinto (M'99) was born and educated in Italy.

Winner of national competitions, he was appointed Assistant Professor of Electromagnetics in 1983, Associate Professor in 1987, and Full Professor in 1990. He has been a faculty member in the Universities of Naples, Salerno (where he founded and chaired the Ph.D. program in Information Engineering from 1993 to 2001), Catania, and Sannio at Benevento, where he is currently the Dean of the Information Engineering Curricula Committee. He has visited several research institutions as an invited lecturer, including CERN, KEK, and NIST (former NBS). In 1998, he was an EU Senior Visiting Scientist at the National Astronomical Observatory, Tokyo, Japan, in connection with TAMA300 experiment. He authored or co-authored more than 100 technical papers in peer-reviewed international journals. His research interests span from electrophysics to gravitational wave experiments.

Dr. Pinto is a Member of the American Physical Society.

Leopold B. Felsen (S'47–M'54–SM'55–F'62–LF'90) was born in Munich, Germany, on May 7, 1924. He received the B.E.E., M.E.E, and D.E.E. degrees from the Polytechnic Institute of Brooklyn, Brooklyn, NY, in 1948, 1950, and 1952, respectively.

He emigrated to the United States in 1939 and served in the U.S. Army from 1943 to 1946. After 1952 he remained with the Polytechnic (now Polytechnic University), becoming University Professor in 1978. From 1974 to 1978 he was Dean of Engineering. In 1994 he resigned from the full-time Polytechnic faculty and was granted the status of University Professor Emeritus. He is now Professor of aerospace and mechanical engineering and Professor of electrical and computer engineering at Boston University, Boston, MA (part-time). He is the author or coauthor of more than 350 papers and of several books, including *Radiation and Scattering of Waves* (Piscataway, NJ: IEEE Press, 1994). He is an Associate Editor of several professional journals and was an Editor of the Wave Phenomena Series (New York: Springer-Verlag). His research interests encompass wave propagation and diffraction in complex environments and in various disciplines, high-frequency asymptotic and short-pulse techniques, and phase-space methods with an emphasis on wave-oriented data processing and imaging.

Dr. Felsen is a Member of Sigma Xi and a Fellow of the Optical Society of America and the Acoustical Society of America. He has held named Visiting Professorships and Fellowships at universities in the United States and abroad, including the Guggenheim in 1973 and the Humboldt Foundation Senior Scientist Award in 1981. In 1974 he was an IEEE Antennas and Propagation Society (APS) Distinguished Lecturer. His "Poet's Corner" appears sporadically in the IEEE/APS Magazine. He received the IEEE/APS Best Paper Award for 1969 and was best paper co-author for 1974 and 1981. He was a contributing author to papers selected for the R. W. P. King Award for 1984, 1986, and 2000. He received the Balthasar van der Pol Gold Medal from the International Union of Radio Science (URSI) in 1975, an Honorary Doctorate from the Technical University of Denmark in 1979, the IEEE Heinrich Hertz Gold Medal for 1991, the APS Distinguished Achievement Award for 1998, the IEEE Third Millennium Medal in 2000, an honorary Laurea degree from the University of Sannio in Benevento, Italy in 2003, the IEEE Electromagnetics Award for 2003, an honorary doctorate from the Technical University of Munich, Germany in 2004, three Distinguished Faculty Alumnus Awards from Polytechnic University, and an IEEE Centennial Medal in 1984. In 1977, he was elected to the National Academy of Engineering. He served on the APS Administrative Committee from 1963 to 1966 and was Vice Chairman and Chairman for both the US (1966–1973) and the International (1978–1984) URSI Commission B.